Calibration procedure for spherical discrete elements using a local moment law

Jean-Patrick Plassiard, Noura Belheine, Frédéric-Victor Donzé

Grenoble Universités
Laboratoire Sols, Solides, Structures et Risques (3S-R)
Domaine Universitaire- BP 53
38041 Grenoble cedex 9 France

Abstract

By using spherical discrete elements, computational costs can be kept low even for large numbers of elements. However, this oversimplification of the granular geometry has drawbacks when quantitatively assessing the model even for frictional geomaterials. To overcome this limitation, the local constitutive law must at least take into account the transfer of a moment between elements. This moment, which is added to normal and shear local interaction forces, increases the number of local parameters. Moreover, when local plastic thresholds are considered, the calibration of the model becomes tricky. With such a set of local parameters, a calibration procedure is proposed, which attempts to tackle the respective role of each parameter in the macroscopic behavior. For this purpose, a series of numerical simulations of triaxial compression tests has been done to check the capability of this model to get good quantitative results.

Introduction

When a DEM model is used, the issue of the modeling scale has to be addressed: the DEM is well adapted to the modeling of granular material, where an element represents a grain (Thornton 2000, Sibille et al. 2005). Thus, numerous authors have used the DEM to simulate granular materials at the heterogeneity scale (Donzé & Bernasconi 2004, Shiu et al. 2006), i.e. the size of an element is on the order of the size of the biggest heterogeneity. This approach gives interesting insights in the local behavior, but makes the modeling of real structures difficult because of the computational cost. Another way to use the DEM consists in using a higher scale model (a mesoscopic scale), which considers that a discrete element represents a large amount of granules. By doing so, the local parameters must be chosen to predict the macroscopic behavior of the geomaterial.

To keep the calculation cost as low as possible, spherical discrete elements are widely used. Because of the rotational invariance of spherical elements, the numerical implementation of the contact detection algorithm remains simple. The main drawback of using spherical geometry is that excessive rolling occurs during shear displacement (Mahboubi et al. 1996). Such models underestimate the value of the friction angle as compared to real geomaterials. While keeping the simplicity of the spherical geometry of elements, it is possible to act upon this rolling by blocking rotations. In triaxial compression simulations, only sliding will then occur, which in turn, will result in a better value of the friction angle (Calvetti et al. 2003). This extreme option gives good results for axial loading, however for shear loading, the

rolling process cannot be ignored (Oda et al. 1982). A moment transfer has been added to the local constitutive law of DEM for biaxial tests (Iwashita and Oda 1998) to keep the advantages of the spherical geometry. Starting from this two-dimensional approach, the formulation of the moment transfer law has been extended here for the three-dimensional case.
This moment, which is added to normal and shear local interaction forces, increases the number of local parameters. With such a set of local parameters, a calibration procedure is proposed, which takes into account the respective role of each parameter in the macroscopic behavior. A series of numerical simulations of triaxial compression tests has been done to check the capability of this model to get good quantitative results. Note that in this work, only the moment transfer will be considered and the torque transfer will be neglected.

Formulation of the model

Let two spheres *A* and *B*, be in contact. The radii of these spherical elements are r_A and r_B. In the global set of axes, their positions are defined by two vectors $\mathbf{x}_A$ and $\mathbf{x}_B$. The interaction force vector $\boldsymbol{F}$ which represents the action of element *A* on element *B* may be decomposed into a normal and a shear vector F^n and F^s respectively, which may be classically linked to relative displacements, through normal and tangential stiffnesses, k^n and k^s.

$$k^n = F_i^n = k^n u^n n_i ,$$

$$\Delta F_i^s = -k^s \Delta u_i^s ,$$

where u^n is the relative normal displacement between two elements, ΔU^s is the incremental tangential displacement and n is the normal contact vector. The shear force F^s is obtained by summing the ΔF^s increments. The normal and tangential stiffnesses are given by:

$$k^n = r \frac{K_A^n . K_B^n}{K_A^n + K_B^n}$$

$$k^s = r \frac{K_A^s . K_B^s}{K_A^s + K_B^s} ,$$

where K_A^n, K_A^s, K_B^n, K_B^s define the input values of normal and tangential stiffnesses for both elements A and B of a contact. r corresponds to the mean value of the two radii.
To reproduce the behavior of non cohesive geomaterials, a Mohr-Coulomb rupture criterion is used:

$$\left\| F^s \right\| \le \left\| F^n \right\| \cdot \tan \mu ,$$

where μ is the "internal" friction angle.

Let k^r be the rolling stiffness. If an isotropic rolling behaviour is assumed, this value is a scalar. The elastic moment $\mathbf{M}_{elast}^L$ created by the rolling part in a local set of axes *L* is written as:

$$\mathbf{M}_{elast}^L = k^r \boldsymbol{\theta}_r^L ,$$

where $\boldsymbol{\theta}_r^L$, the angular vector of the rolling part in the set of axes L.

The rolling stiffness parameter k^r defines the level of influence that the resistant moment produces; Let's introduce a dimensionless number β_r which expresses a relationship between k^r and k^s, such that,

$$\beta_r = \frac{k^r}{k^s r^2}$$

Let’s also introduce η_r as a dimensionless parameter which controls the elastic limit of rolling. If $\|\mathbf{F}_n\|$ represents the norm of the normal force at the contact point, the elastic limit is given by the plastic moment vector $\mathbf{M}^L_{plast}$ such that:

$$\mathbf{M}^L_{plast} = \eta_r r \|\mathbf{F}_n\|.$$

Thus, rolling moment $\mathbf{M}_r$ is given by:

$$\mathbf{M}_r = m_{L\_G}\ \min\left(\left\|\mathbf{M}^L_{elast}\right\|;\left\|\mathbf{M}^L_{plast}\right\|\right)\frac{\mathbf{M}^L_{elast}}{\left\|\mathbf{M}^L_{elast}\right\|}$$

where m_{L_G} defines the transition matrix from the local set of axes L to the global set of axes G.

Calibration of the local parameters

The calibration of the local properties of the numerical model to the properties of a real geo-material is conveniently done by comparing a simulated and a real triaxial test. Once calibrated, the predictive capabilities of the numerical model will be checked by simulating other triaxial tests. For the calibration step, the selected local parameters are: K^n, K^s, k^r (or β_r), μ and η_r. Their values will be fixed to reproduce, not only the correct shapes of stress-strain and the volumetric curves, but also the correct macroscopic values of Young’s modulus E, Poisson’s ratio ν, the dilation angle ψ, the peak σ_{peak} and the post peak strength $\sigma_{post-peak}$, see Figure 1.

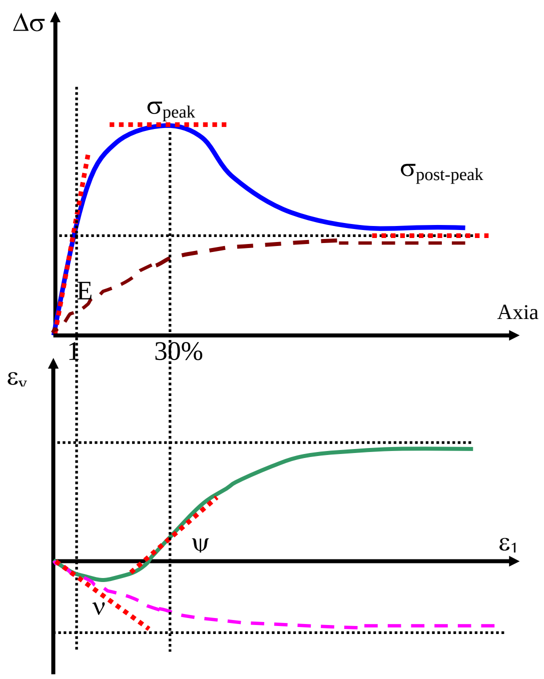

Figure1. Typical responses obtained with triaxial tests for dense (solid lines) and loose (dashed lines) sands.

To do so, one must identify the influence of each local parameter on the macroscopic response. First it was found that the elastic parameters and the rupture parameters can be calibrated separately, which is in agreement with previous results (Calvetti et al. 2003, Sibille et al. 2006).

The local elastic parameters K^n and K^s play a major role in the elastic response. The other elastic parameter β_r has a lower impact (less than 10%) on Young's modulus E and Poisson's ratio ν. Thus, K^n and K^s will be set first to calibrate the macroscopic elastic behavior.

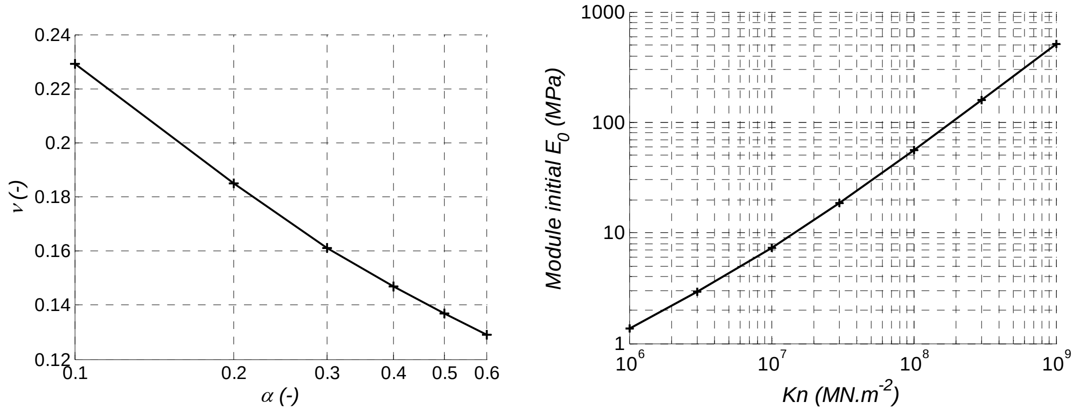

Figure 2. On the left, dependency of Poisson's ratio on the ratio $\alpha = K^s / K^n$, on the right, dependency of Young modulus on K^n.

For an arbitrary value of K^n, K^s is set according to chosen value of Poisson's ratio. Then, for a constant $\alpha = K^s / K^n$, K^n is set such that the desired value of Young's modulus is obtained (Figure 2).

Once the local elastic parameters are set, the values of the other local parameters (μ, a_S, β_r and η_r) must be determined. First, the local friction angle μ has a major influence on both the peak stress and the dilatancy angle, but a low one on the residual stress (Figure 3). Because of the low influence of β_r on the dilatancy angle, as it will be seen, μ <u>is chosen to control the dilatancy angle value</u>.

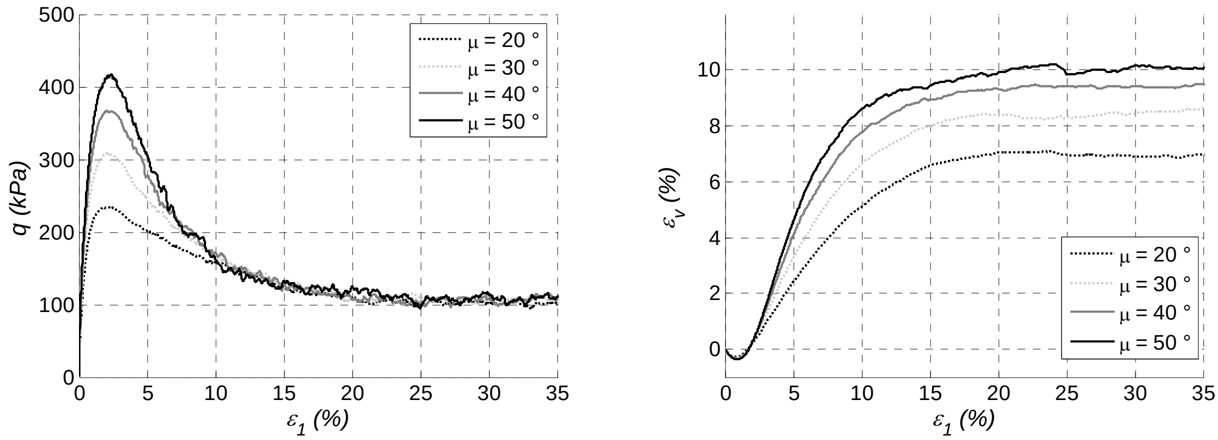

Figure 3. Dependency on the value of local friction angle: on the left, deviator stress-strain curves, on the right, volumetric-strain curve.

Then, it is observed that β_r has little influence on the dilatancy angle (Figure 4), which confirms that using μ to control this macroscopic parameter is an adequate choice. On the other hand, β_r highly affects the stress peak and the residual peak. Then, because of the low influence of η_r and μ on the residual peak, as it will also be seen, β_r is chosen to control the residual peak value.

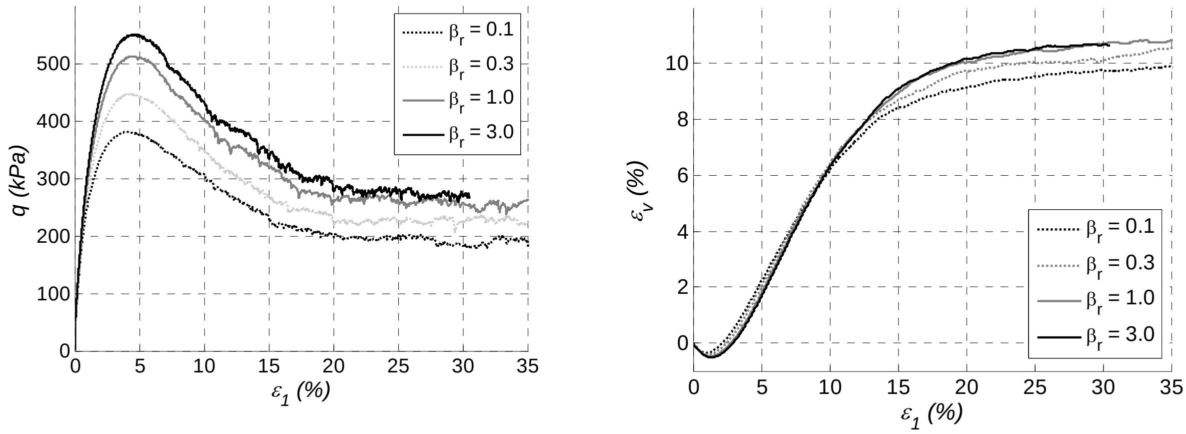

Figure 4. Dependency on the value of the dimensionless rolling stiffness parameter: on the left, deviator stress-strain curves, on the right, the volumetric-strain curve.

Finally, η_r has little influence on both the residual stress value and the dilatancy angle (Figure 5), so that μ and β_r can be kept to set these macroscopic values. Fortunately, η_r affects the stress peak. Consequently, η_r can be chosen to set the peak stress value.

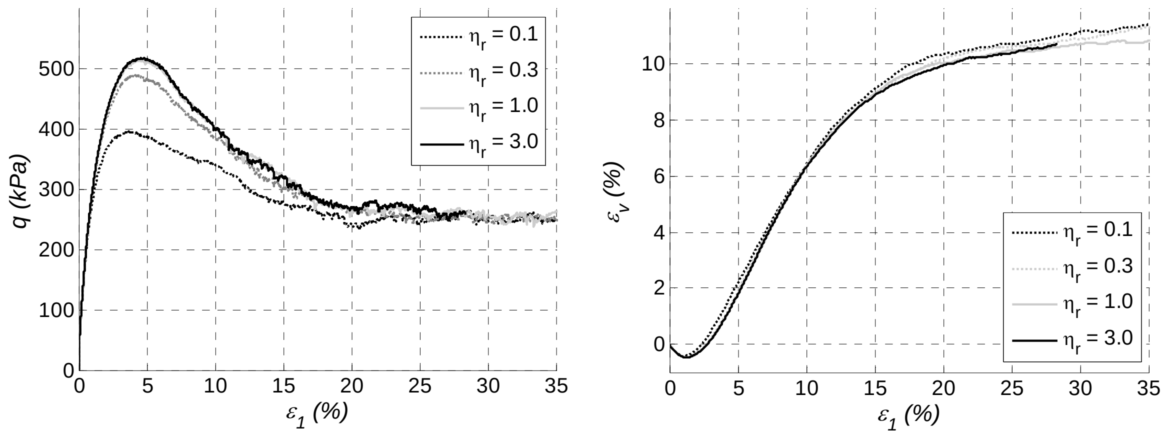

Figure 5. Dependency on the value of the elastic limit of rolling: on the left, of deviator stress-strain curves, on the right, the volumetric-strain curve.

Application case: predicting the behavior of a granular material

As a calibration example, the numerical modeling has been used to simulate the response of the "Labenne" sand (Canepa and Depresles 1990). The soil of Labenne is made of sand from a dune and its properties are given in Table A.

Young's modulus E, *Mpa*	96.0
Poisson's ratio, ν	0.28
Friction angle, φ °	36.50
Dilation angle, ψ °	11.4
Cohesion, *kPa*	0.0
Porosity, *%*	40.0
Density, KN/m^3	16.6

Table A. Properties of the "Labenne" sand

The triaxial test was modeled using SDEC (Donzé and Magnier 1995, 1997) by confining a dense discrete element medium within six smooth walls. The consolidation took place under gravity-free conditions, so that the 10 000 discrete elements arrangement was considered to be almost isotropic (Figure 6). The top and bottom boundaries moved vertically as loading platens, either under force-controlled condition or under strain-controlled conditions. Lateral boundaries simulate the confining pressure experienced by the sample sides. In the numerical simulation, the sample is loaded in a strain-controlled mode by specifying the velocities of the top and the bottom walls. To this end, it can be noted that since the walls are frictionless, any friction between the sample and the loading platens is avoided, hence allowing the wall applied stresses to remain normal to each wall.

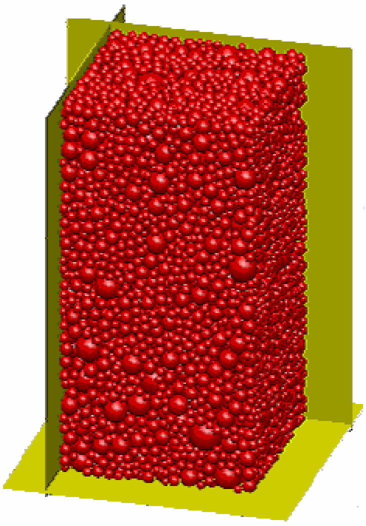

Figure 6. Numerical specimen of 10 000 discrete elements representing the triaxial test for the "Labenne" sand

During all test steps, displacements of the lateral walls are controlled automatically by a servo mechanism that maintains a constant confining stress within the sample. According to the given boundary conditions, the stress and strain states within the sample are assumed to be homogeneous. Strains are then calculated directly from wall displacements, while the corresponding stresses are obtained from boundary forces, as in conventional laboratory testing.

Thus, for a confining pressure of 100 kPa, the local parameters, K^n, K^s, K^r (or β_r), μ and η_r were chosen to fit the stress-strain and the volumetric curves (Figure 7). Laboratory tests are available under different confining pressures (100, 200 and 300 kPa). The corresponding values of the local parameters can be found in Table B.

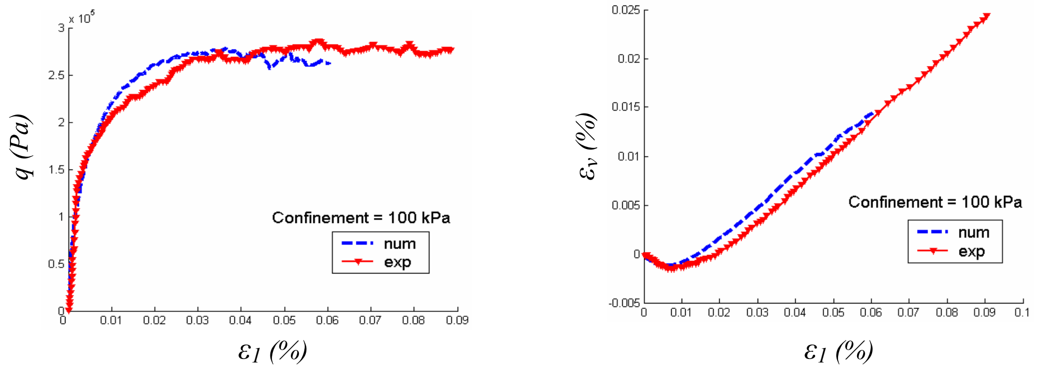

Figure 7. Curves obtained from the calibration procedure for a confining pressure of 100 kPa

Parameters	Average value
Normal contact stiffness K^n,	9.6 x 10^8
Ratio $\alpha = \dfrac{K^s}{K^n}$,	0.04
Inter-particle friction angle μ °,	30.0
Rolling stiffness parameter β_r,	0.12
Dimensionless parameter η_r,	1.0

Table B. Local parameter values of the numerical model.

Figure 8 shows the numerical results obtained with the parameters reported in Table C for confining pressures of 200 and 300 kPa. The results indicate that the non linear stress-strain behavior of sand including dilatancy is covered by the numerical model. This shows that the model can be used as a predictive tool.

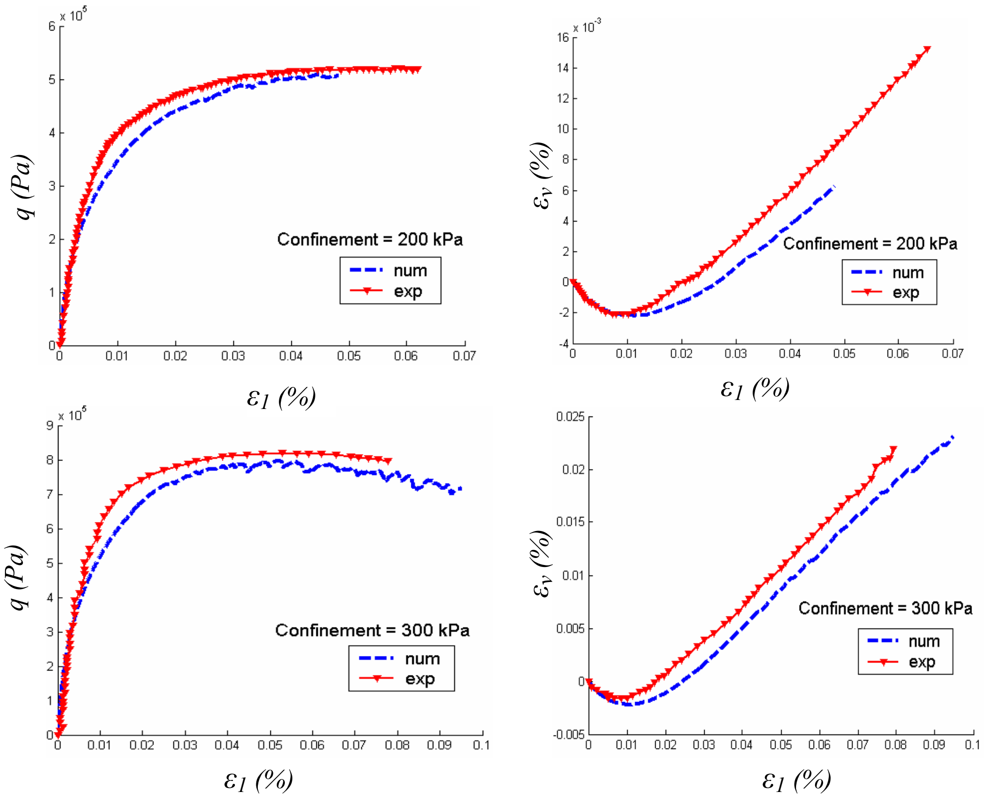

Figure 8. Predictive curves obtained for confining pressures of 200 kPa and 300 kPa

Conclusion

Simulations with the discrete element method have been presented. Spherical elements were used because the corresponding simulation algorithm is simple and fast. Because classical DEM have difficulties to deal with the shearing mode because of the high rolling ability of the spherical elements, a transfer moment law is used. Based on this, a calibration procedure was proposed, which attempted to consider the respective role of each local parameter in the macroscopic behavior. Numerical tests were carried out to simulate laboratory tests of "Labenne" sand. To do so, the calibration methodology was first used, before using the model as a predictive tool. In spite of its simplicity, the numerical model was able to reproduce the main features of the triaxial tests. In terms of the deformational characteristics, a good agreement between the numerical and real tests was obtained. The corresponding shear strength parameters agreed well. Finally, the predictive results were in good agreement with the experimental results, even if the numerical medium was made of a small amount of spherical elements (around 10 000).

Bibliography

Canepa Y, Depresles D. Fondations superficielles. Essais de chargement de semelles établies sur une couche de sable en place, station expérimentale de Labenne. Influence des conditions d'excution, Compte rendue des essais 1990, FAER 1. 17.02.09., 1990.

Calvetti F., Viggiani G., Tamagnini C., « A numerical investigation of the incremental non-linearity of granular soils », *Rivista Italiana di Geotecnica, Special Issue on Mechanics and Physics of Granular Materials*, 2003.

Donzé, F. & Magnier S-A., Formulation of a three-dimensional numerical model of brittle behavior, *Geophys. J. Int.*, 122, 790-802. 1995.

Donzé F-V, Magnier S-A. Spherical Discrete Element Code. *Discrete Element Project Report N° 2.GEOTOP*. Université du Québec à Montréal, 1997.

Donzé, F. V. & P. Bernasconi, Simulation of the Blasting Patterns in Shaft Sinking Using a Discrete Element Method, *Electronic Journal of Geotechnical Engineering* vol:9 No B, 2004.

Iwashita K., Oda M. (1998). "Rolling resistance at contacts in simulation of shear band development by DEM." *Journal of Engineering Mechanics*, 124(3), 285-292.

Mahboubi A., Ghaouti A., Cambou B. (1996), « La simulation numérique discrète du comportement des matériaux granulaires », revue française de géotechnique, n° 76, p.45-61.

Oda M., Konishi J., Nemat-Nasser S. (1982). "Experimental micromechanical evaluation of strength of granular materials: effect of particle rolling." *Mechanics of Materials*, 1, 269-283.

Shiu, W, F.V. Donzé and S.A. Magnier, Numerical study of rockfalls on covered galleries by the Discrete Elements Method, Electronic Journal of Geotechnical Engineering, vol:11 No D, 2006.

Sibille, L., F. Nicot, F.V. Donzé and F. Darve, Material instability in granular assemblies from fundamentally different models, *International Journal For Numerical and Analytical Methods in Geomechanics*, DOI: 10.1002/nag.591, 2007.

Thornton, C., Numerical simulations of deviatoric shear deformation in granular media, *Geotechnique*, Vol. 50 No.4, pp.43-53, 2000.